

# Design and implementation of multi robot research platform based on UWB

Lv Qiang<sup>1</sup>, Wei Heng<sup>1</sup>, Lin Huican<sup>1</sup>, Zhang Ying<sup>1</sup>

1. Department of control engineering, The Academy of Armored Forces Engineering, Beijing 100072, China

E-mail: wh\_killer@foxmail.com

**Abstract:** Based on the ultra wideband (UWB) technology in the Ubuntu robot operating system (ROS) framework to build a centralized distributed multi robot research platform. Based on the UWB chip, a bidirectional ranging module is designed, and the singular value removal module based on the minimum covariance determinant (MCD) Mahalanobis distance detection algorithm is designed for the singular values in the ranging process. The extended Kalman filtering optimization module is designed to solve the problem of excessive coordinate jump and edge effect in three edge location algorithm. ROS communication network is constructed based on multi master design, and the entry and exit mechanism, so that when a robot failure will not affect the operation of the whole system or after the completion of the task can exit the system to reduce the burden of the central processor. Finally, the kinematics and dynamics model of omni-directional robot based on the design of inverse dynamic compensation control strategy of synovial control combining with PID control, and complete the single robot trajectory tracking experiment and multi robot formation mission experiment.

**Key Words:** UWB; multi-robot system; Mahalanobis distance; omnidirectional robot; trajectory tracking

## 1 Introduction

In recent years, more and more researches on autonomous mobile robots have been made, and the precise localization of robots in the environment has become a research hotspot. In outdoor broad environment, the research of autonomous navigation system based on GPS and IMU fusion has been more mature<sup>[1][2]</sup>. But with the robot application environment more and more complex, more and more higher precision, especially in the interior, the forest, the airport GPS by signal interference suppression, the environment, and how to realize the accurate positioning of the robot autonomous navigation has become the research frontier. For indoor navigation, more recent research is robot SLAM algorithm<sup>[3][4]</sup>, especially IMU and laser fusion algorithm<sup>[5][6]</sup> and fusion algorithm for visual and IMU<sup>[7][8]</sup>, but all of these algorithms only provide local coordinates of the robot, when converted to global coordinates, IMU due to the cumulative error factors and the influence of exercise on sensor measurement the data will appear, the measurement accuracy is not enough, especially when based on the multi robot system<sup>[3]</sup>, the complexity of the algorithm is greatly improved, real-time performance is also affected. Secondly, cameras, laser rangefinder and other sensors, large volume and weight, does not apply to the mobile robot is becoming smaller and smaller trend.

Compared with a single robot, the multi robot system has better fault tolerance and redundancy, and its application prospect is very broad<sup>[9]</sup>. Different from ultrasonic or laser ranging, ultra wideband (Ultra Wideband UWB) technology can penetrate walls and forest, compared to the traditional narrowband RF signal, the frequency response can reach more than 10Hz, high time resolution, anti multipath ability, strong penetrating ability, is advantageous to the indoor real-time positioning of the robot<sup>[10]</sup>. I study the knowledge, has not found the relevant literature UWB the development of autonomous navigation system of multi robot based on domestic, so this paper based on the laboratory research of mature based omni-directional robot<sup>[11]</sup>, the platform is

designed for multiple mobile robots based on UWB, and completed the trajectory tracking, formation control and other projects, for the following multi sensor fusion, multi robot SLAM heterogeneous robot cooperative control, multi robot cooperative control algorithm research foundation.

## 2 UWB real time location system

The real-time positioning system based on DecaWave's new UWB measurement chip DW1000<sup>[12]</sup> as the base, to construct the real-time positioning system 4 anchor, multi label (Real-Time Location, Systems, RTLS)..

### 2.1 Two-way time-of-flight ranging, TW-ToF

Two-way ranging algorithm is in the anchor and the label are mounted on the receiver and transmitter, through two-way ranging can eliminate clock error and offset error, get more accurate location results, the algorithm is shown in figure 1.

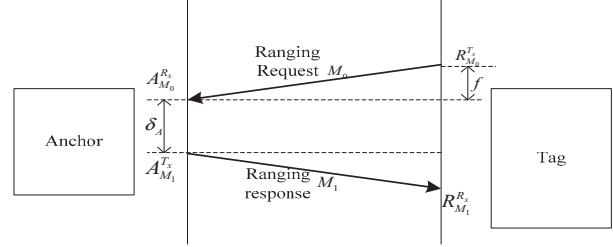


Fig.1 two-way ranging algorithm

In real-time positioning system development, the label placement on the robot, requested by the label to send to the anchor anchor location, after receiving the request signal, it automatically sends a response signal. As shown in Figure 1, we can see that the two UWB modules are not symmetrical. When the label is positioned on the robot send the request signal  $M_0$  at the time  $R_{M_0}^{T_x}$ . an anchor after the time  $f$  at

$A_{M_0}^{R_x}$  received the pulse. At the time  $\delta_A$ , calculate the frontier offset error, then the anchor transmits a response signal at  $A_{M_1}^{T_x}$ , the tag after time  $f$  at  $R_{M_1}^{R_x}$  received a

response signal. Between the tag and the anchor transmission time  $f$ , can be expressed as

$$f = \frac{(R_{M_1}^{R_s} - R_{M_0}^{T_s} - \delta_A)}{2} \quad (1)$$

The distance between the tag and the anchor is

$$d_{RA} = f \cdot c \quad (2)$$

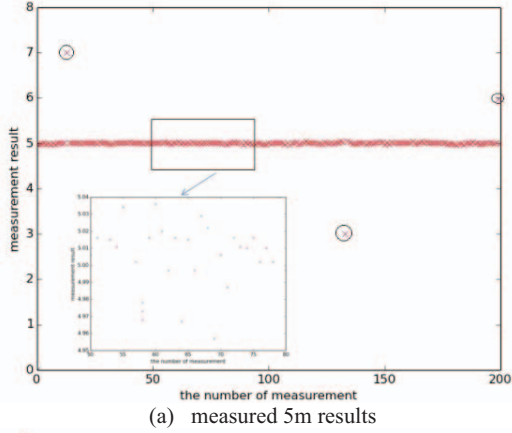
Which  $c = 3 \times 10^8$  m/s for electromagnetic wave propagation velocity in the air.

In the ranging experiment, the measurement environment is shown in figure 2.

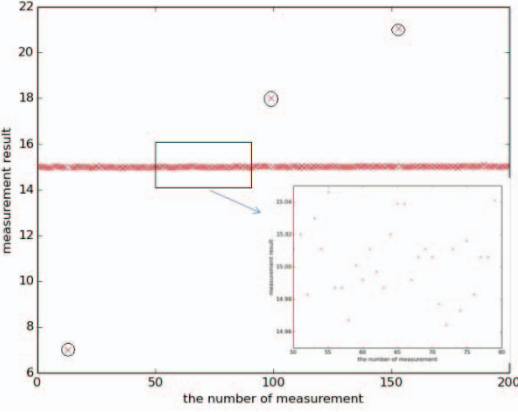


Fig.2 experimental environment of distance measurement

Experiments were selected 5m, 15m three points for measurement, the results shown in Figure 3



(a) measured 5m results



(b) measured 15m results

Fig.3 measured results of two-way ranging algorithm

From the experiment, the ranging accuracy between  $\pm 5\text{cm}$ , achieve the accuracy of indoor positioning robot requirements, response time at 5ms, enough robots to

complete the corresponding control. But in the course of the experiment, we find occasional outliers (the points in the small black circle in the picture). The emergence of outliers will have a great impact on the following robot positioning, trajectory tracking, and even the robot out of control and other responses, so in the next section design singular value removal module.

## 2.2 Singular value removal module

In view of the singular value of UWB ranging occasionally, the improved Mahalanobis distance singular value detection algorithm is adopted to deal with this problem. The traditional Mahalanobis distance outlier detection algorithm using the sensor data directly to the mean and the covariance matrix of Mahalanobis distance calculation, calculated results may not be robust, vulnerable to the singular value affect shielding effect, leading to the normal data and the singular value of Mahalanobis distance difference calculated, thus unable to remove the singular value. Based on the minimum covariance determinant (Minimum covariance determinant, MCD) estimation of Mahalanobis distance outlier detection algorithm, using the mean and covariance matrix estimator is calculated in MCD estimation of sound, there is a big difference between the Mahalanobis distance and singular value of normal data, so as to achieve the detection and removal of abnormal value function.

The formula for mahalanobis distance

$$dT(i) = \sqrt{(x_i - T)^T S^{-1} (x_i - T)} \quad (3)$$

In the formula,  $T$  is mean,  $S$  is covariance matrix. The obtained Mahalanobis distance approximation obeys the chi square distribution with degrees of freedom of  $P$ , Set threshold under certain confidence  $\sqrt{x_{p,\alpha}^2}$ , at  $d(i) > \sqrt{x_{p,\alpha}^2}$  it is a singular value<sup>[13]</sup>.

FAST-MCD algorithm and Mahalanobis distance MCD detection algorithm using Rousseeuw P is proposed based on the robust mean and covariance matrix by iteration, and then calculate the robust Mahalanobis distance, finally the singular value detection<sup>[14]</sup>. Algorithm flow chart is shown in figure 4.

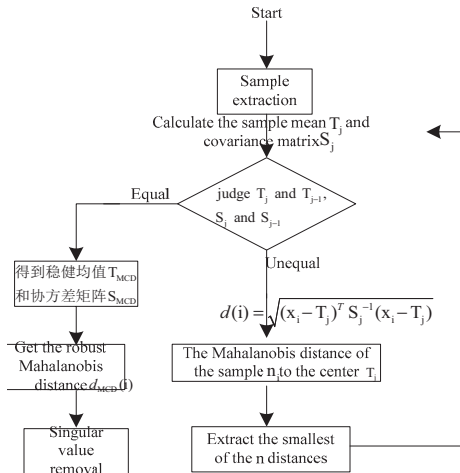


Fig.4 flow chart of Mahalanobis distance singular value detection algorithm based on MCD

Experiment, still choose 5m, 15m three points for measurement, the results shown in figure 5.

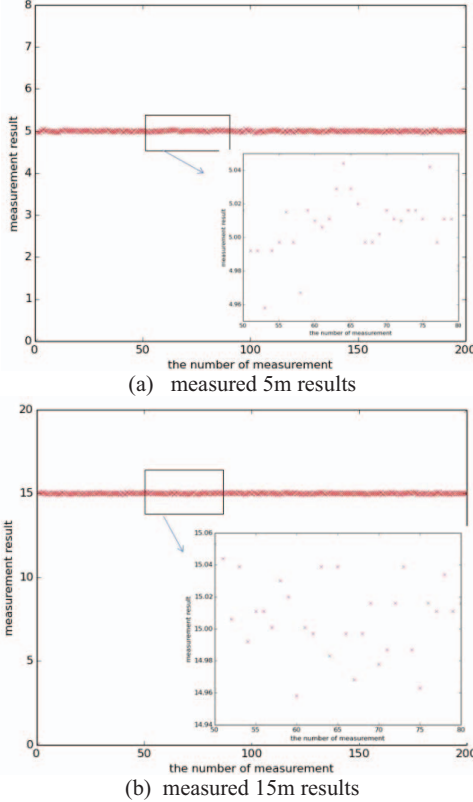


Fig.5 based on robust Mahalanobis distance ranging results after the removal of singular value

It can be seen from the experiments that the singular value removal module based on robust Mahalanobis distance can remove the singular values which occur occasionally in the ranging process, and achieve the design requirements.

### 2.3 Position measurement module

Taking into account the UWB module can get more accurate distance between the highlights, and because the three side measurement (Trilateration) calculation is small and easy to achieve, so the system uses the algorithm for location calculation. In order to improve the measuring accuracy, the system adopts 4 anchor, at the same time, taking into account the current only for the ground mobile robot, in order to reduce the complexity of the algorithm, the anchor in the same level.

The known anchor coordinates for the location coordinates  $(x_1, y_1, z), (x_2, y_2, z), (x_3, y_3, z), (x_4, y_4, z)$ , unknown points  $(x_0, y_0)$ , and the distance from unknown points to three known points  $d_1, d_2, d_3, d_4$ , obtaining the following formula

$$\begin{cases} (x_1 - x_0)^2 + (y_1 - y_0)^2 + z^2 = d_1^2 \\ (x_2 - x_0)^2 + (y_2 - y_0)^2 + z^2 = d_2^2 \\ (x_3 - x_0)^2 + (y_3 - y_0)^2 + z^2 = d_3^2 \\ (x_4 - x_0)^2 + (y_4 - y_0)^2 + z^2 = d_4^2 \end{cases} \quad (4)$$

In this system, the anchor coordinates is  $(0, 0, 0.72)$ ,  $(3.8, 0, 0.72)$ ,  $(3.8, 2.4, 0.72)$ ,  $(0, 2.4, 0.72)$ , respectively. Then

$$\begin{cases} x_{01} = (3.8 \times 3.8 - d_2 \times d_2 + d_1 \times d_1) / 7.6 \\ x_{02} = (3.8 \times 3.8 - d_3 \times d_3 + d_4 \times d_4) / 7.6 \end{cases} \quad (5)$$

$$\begin{cases} y_{01} = (2.4 \times 2.4 - d_4 \times d_4 + d_1 \times d_1) / 4.8 \\ y_{02} = (2.4 \times 2.4 - d_3 \times d_3 + d_2 \times d_2) / 4.8 \end{cases} \quad (6)$$

Then

$$\begin{cases} x = (x_{01} + x_{02}) / 2 \\ y = (y_{01} + y_{02}) / 2 \end{cases} \quad (7)$$

In the experiment, 2 groups of coordinates are measured, the 1 group is near the axis boundary, one group is the general point, as shown in figure 6.

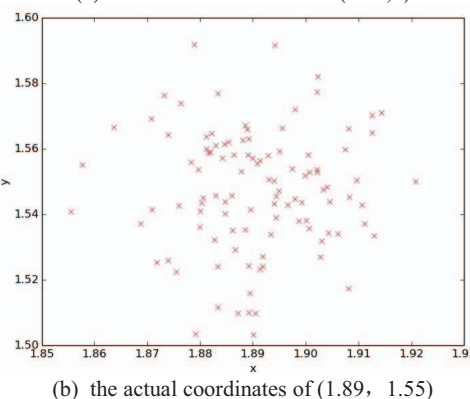
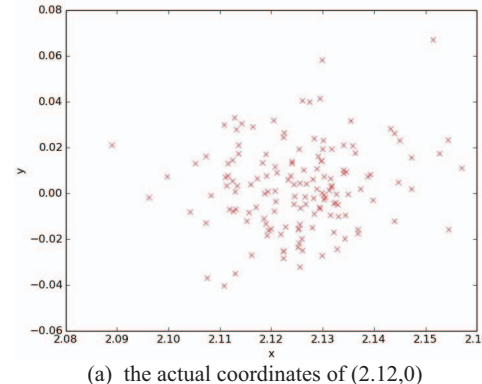


Fig.6 measured results of Trilateration algorithm

Experiments show that x, y coordinate measurement is accurate, general point measurement error is  $\pm 4\text{cm}$ . But at the point near the axis boundary, the error becomes larger  $\pm 8\text{cm}$ , The main reason is that the three side measurement method will enlarge the influence of UWB ranging error at the boundary. Aiming at the general point error and edge effect, an optimized module based on extended Calman filtering algorithm is designed to optimize the coordinates.

### 2.4 Optimization module

The extended Calman filter algorithm is used to design the optimization module to solve the problem of large coordinate jump. The extended Calman filtering algorithm is an on-line nonlinear model, which is based on the principle of Calman filtering to deal with the nonlinear filtering problem. Algorithm schematic shown in figure 7.

---

Algorithm: Extended Calman filter optimization

input: t-1 moment state:  $(x, y)_{t-1}, S_{t-1}$   
t moment state control signal:  $u_t$   
t moment state observed value:  $z_t$

output: t moment state:  $(x, y)_t, S_t$

- 1: predict( $(x, y)_{t-1}, S_{t-1}, u_t \rightarrow ((x, y)_t^-, \bar{S}_t)$
  - 2: update( $((x, y)_t^-, \bar{S}_t, z_t) \rightarrow ((x, y)_t, S_t)$
  - 3: return  $(x, y)_t, S_t$
- 

Fig.7 EKF optimization algorithm schematic

Among them, the function predict () and update () is the standard procedure for Calman filtering, predict ():

$$\hat{x}_t = A_{t-1} \hat{x}_{t-1} \quad (8)$$

$$S_t^- = A_{t-1} S_{t-1} A_{t-1}^T + Q_{t-1} \quad (9)$$

update()为:

$$\begin{cases} \hat{d}_t = \|\hat{S}_t^- - S^N\| \\ H_t = \frac{1}{\hat{d}_t} [(\hat{S}_t^- - S^N)^T \ 0] \end{cases} \quad (10)$$

$$K_t = S_t^- H_t^T (H_t S_t^- H_t^T + R)^{-1} \quad (11)$$

$$\hat{x}_t = \hat{x}_{t-1} + K_t (d_t - \hat{d}_t) \quad (12)$$

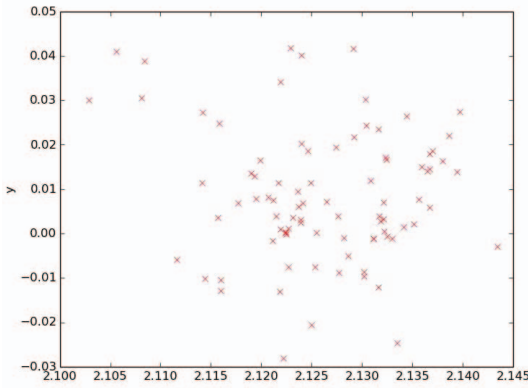
$$S_t = (I - K_t H_t) S_t^- \quad (13)$$

Among them,  $x = \begin{pmatrix} S \\ T \end{pmatrix}$ ,  $A_k = \begin{pmatrix} I & \Delta t I \\ 0 & I \end{pmatrix}$ ,

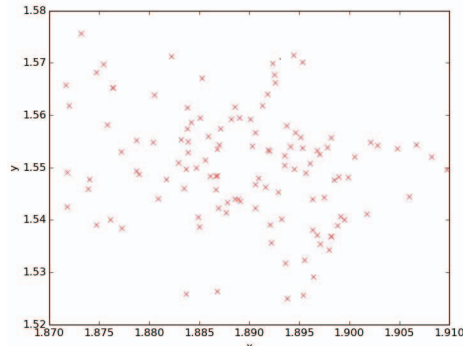
$$Q_t = \begin{pmatrix} \frac{1}{4}(\Delta t)^4 & \frac{1}{2}(\Delta t)^3 \\ \frac{1}{2}(\Delta t)^3 & (\Delta t)^2 \end{pmatrix} \otimes \text{diag}(\sigma_x^2, \sigma_y^2), \quad " \wedge " \text{ is}$$

Estimated value, “-” is priori value.

According to the 2 coordinate positions measured in the previous section, the measurements were carried out and the results were shown in Figure 8. The experimental results show that, by adding the extended Calman filter optimization module, the general point measurement error is reduced to  $\pm 3$  cm, the edge point measurement error is reduced to  $\pm 4$  cm, which meets the requirements of indoor robot autonomous navigation to the position accuracy.



(a) the actual coordinates of (2.12, 0)



(b) the actual coordinates of (1.89, 1.55)

Fig.8 Measured results after EKF algorithm optimization

### 3 Multi robot platform construction

Multi robot cooperative control system is developed on the basis of system (Robot operating system, ROS). The platform adopts modular design, which is convenient for subsequent multi robot system expansion and algorithm research.

#### 3.1 Omnidirectional robot control based on UWB

The kinematics coordinate system of the four wheeled omni-directional robot is shown in figure 9,  $O_w, X_w, Y_w$  is on the basis of the anchor point of the global coordinate system,  $O_r, X_r, Y_r$  is relative coordinate system;  $(x_w, y_w, \theta_w)$  is robot pose in global coordinate system,  $(x_r, y_r, \theta_r)$  is robot pose in relative coordinate system;  $(v_1, v_2, v_3, v_4)$  is robot wheel line speed,  $\theta$  is azimuth, L is distance from the wheel to the center of mass.

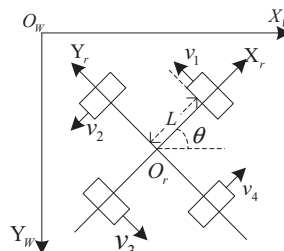


Fig.9 kinematics coordinate system of four wheeled omnidirectional robot

Obtaining the kinematics model of four wheeled omni-directional robot :

$$\begin{bmatrix} v_1 \\ v_2 \\ v_3 \\ v_4 \end{bmatrix} = \begin{bmatrix} -\sin \theta & -\cos \theta & L \\ -\cos \theta & \sin \theta & L \\ \sin \theta & \cos \theta & L \\ \cos \theta & -\sin \theta & L \end{bmatrix} \begin{bmatrix} \dot{x}_w \\ \dot{y}_w \\ \dot{\theta}_w \end{bmatrix} \quad (14)$$

Kinetic model:

$$\begin{bmatrix} m & 0 & 0 \\ 0 & m & 0 \\ 0 & 0 & I \end{bmatrix} \ddot{q} = \begin{bmatrix} -\sin \theta & -\cos \theta & \sin \theta & \cos \theta \\ -\cos \theta & \sin \theta & \cos \theta & \sin \theta \\ L & L & L & L \end{bmatrix} \times$$

$$\left( \frac{nK_t}{RR_a} U - \frac{n^2 K_t^2}{RR_a} r \right) \quad (15)$$

$m$  is the total mass of the robot;  $I$  is the rotation inertia of the robot revolves around the center;  $R$  is the wheel radius;  $R_a$  the armature resistance of the motor;  $K_t$  the motor torque constant;  $U = (U_1, U_2, U_3, U_4)^T$  the motor voltage;  $r = (r_1, r_2, r_3, r_4)$  the wheel speed.

Based on the kinematics and dynamics model of omni-directional robot design, the inverse dynamic compensation control strategy of synovial control combining with PID control, the control algorithm described in detail has been published in the literature [11], here no longer repeat. Specific control flow based on UWB as shown in figure 10.

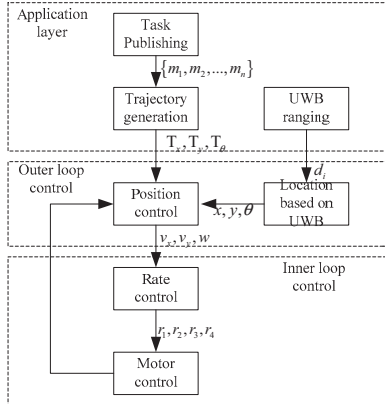


Fig.10 flow chart of omni directional robot autonomous control based on UWB

### 3.2 Multi robot network construction

Because of the open-source robot operating system ROS using distributed processing framework, so that each function can be used in modular design, convenient for later researchers to add a variety of functional modules to their own needs, and coupling with other modules easy in operation, so the design of the system is centralized distributed cooperative control system of multi robot based on ROS development.

The system uses WiFi to connect each robot with the central processor, the central processor through the SSH tool remote login each robot, so as to achieve off board control. Run roscore in the central processor and each robot, each robot includes a central processor as an independent master, this design has two advantages: first, if a robot problems or central processor faults, will not cause the whole operation of multi robot system paralysis or confusion; second: design entry with the exit mechanism, easy to add or reduce the number of robots in the process of operation, such as a robot to complete the assigned task, you can opt out of the multi robot system, this helps to reduce the burden of central processor. Here to build multi robot system, using the ROS master\_discovery and master\_sync two packages, used to add time tags on each robot, and time synchronization. Multi-robot system network diagram shown in figure 11.

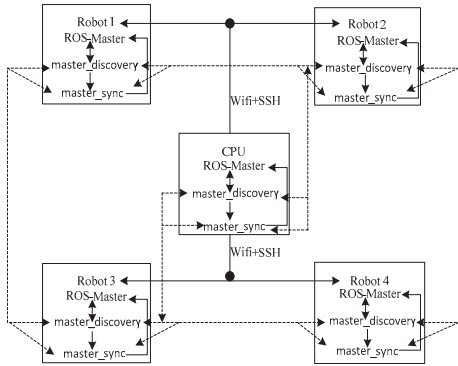


Fig.11 schematic diagram of multi-robot system network  
After the start of the multi robot system, the central processor ROS node figure shown in figure 12.

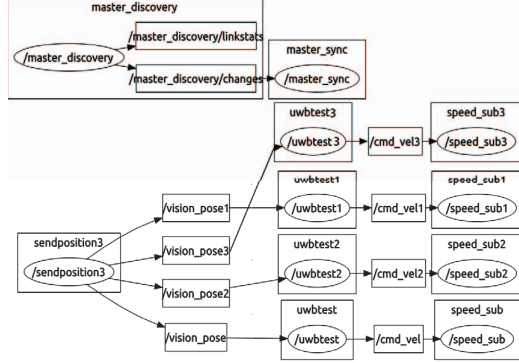


Fig.12 the central processor ROS node graph

## 4 Experiment

Multi robot research platform UWB to build a 4 anchor 4 label based on the whole system using Ubuntu system, ROS platform to build a multi-robot network architecture based on the experimental platform, as shown in figure 13. Based on the system, first of all to do single robot trajectory tracking experiment, the positioning accuracy of UWB control algorithm and the omni-directional robot is verified; secondly, the multi robot formation task experiment, test the positioning accuracy of the communication network of multi robot cooperative control algorithm, multi robot and multi robot under the condition of UWB.

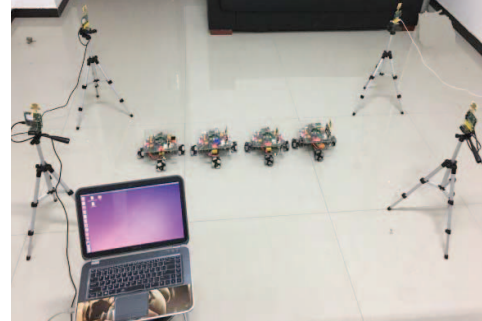


Fig.13 Multi-robot research platform

### 4.1 References

In order to verify the omni-directional robot control algorithm and UWB ranging accuracy, a single robot trajectory tracking experiment is designed. Set robot trajectory function as

$$y=1.25+1.25\times\sin(2\pi x/2.5) \quad (16)$$

It should be noted that, at present, because the robot is not equipped with any other sensors, just rely on UWB system control, so when the robot first boot, the need for initial attitude judgments. Design, let the robot boot after the first body coordinate system X axis direction of 20 cm, and then returned to the ground, so as to determine the robot's initial attitude. The experimental results are shown in figure 14.

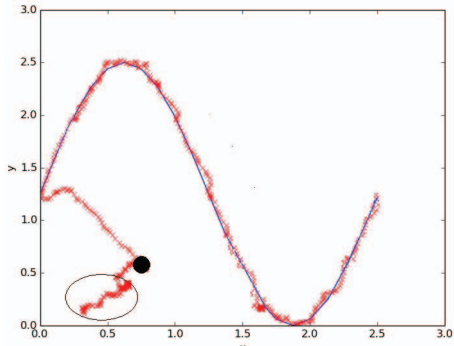


Fig.14 single robot sinx trajectory tracking

As shown in the figure, black spots as the starting position of the robot, the ellipse around the area looking for the initial position for the robot, the blue dashed line to the desired trajectory, the red x point position is UWB measured in real time. As can be seen from the figure, the robot trajectory tracking is good, can better complete the trajectory tracking, to reach the established goal.

#### 4.2 Multi robot formation mission experiment

Multi robot formation control experiment, task release: robot 1, 2, 3 and 4, move to the point (1.0, 0.8), (1.0, 1.8), (3, 1.8), (3, 0.8), respectively. Then tracking circular trajectory, and after the completion of the task automatically withdraw from the multi robot system. The experimental results are shown in Figure 15.

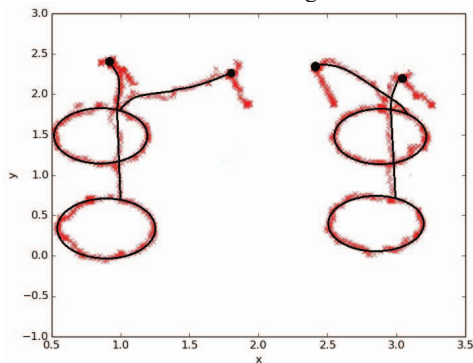


Fig.15 Multi-robot formation mission experiment

The black spot is the starting position of the robot, the black line is the desired trajectory, and the red dot is the location of the UWB measured in real time. Can verification from the experiment that the normal network communication, multi robot, multi robot under the condition of UWB positioning accuracy to meet the requirements of robot navigation, multi robot cooperative control algorithm and control strategy can be verified through the system, and verify the join and exit mechanism.

#### 5 Prospect and summary

Based on UWB, this paper designs a multi robot cooperative control research platform based on omni

directional robot. The software architecture is developed based on ROS framework in Ubuntu. In the use of UWB based on the bidirectional algorithm measurement, for occasional, singular value, singular value is designed for removal of modules, three edge location algorithm, coordinate beating large problem, design optimization module for optimization. Based on the kinematics and dynamics equations of omnidirectional robot, the inverse dynamic compensation control strategy combining the synovial control with PID control is designed and implemented. Finally, the reliability of the multi robot system is verified by single robot trajectory tracking experiment and multi robot formation mission experiment.

Next, can rely on this system, equipped with different sensors, the omni-directional robot such as monocular camera, binocular camera, depth camera, laser range finder sensor, study algorithm and multi robot SLAM algorithm of multi sensor fusion; can also rely on this system, the research on multi robot cooperative control strategy and algorithm; also, rely on this system of heterogeneous robot cooperative control, such as adding aircraft.

#### References

- [1] Sueoka S, Irie T. The study for control of the robot plane with GPS and IMU[J]. Journal of Medical Virology, 2016, 13:417-418.
- [2] Sasani S, Asgari J, Amiri-Simkooei A R. Improving MEMS-IMU/GPS integrated systems for land vehicle navigation applications[J]. GPS Solutions, 2016, 20(1):89-100.
- [3] Saeedi, Sajad, Trentini, Michael, Seto, Mae, et al. Multiple - Robot Simultaneous Localization and Mapping: A Review[J]. Journal of Field Robotics, 2016, 33(1):3-46.
- [4] Othón E J J, Michel D, Gordillo J L. Visual EKF-SLAM from Heterogeneous Landmarks†[J]. Sensors, 2016, 16(4):489.
- [5] Aghili F, Su C Y. Robust Relative Navigation by Integration of ICP and Adaptive Kalman Filter Using Laser Scanner and IMU[J]. IEEE/ASME Transactions on Mechatronics, 2016, 21:1-1.
- [6] Luo W, Wang K C P, Li L. Hydroplaning on Sloping Pavements Based on Inertial Measurement Unit (IMU) and 1mm 3D Laser Imaging Data[J]. Periodica Polytechnica Transportation Engineering, 2016, 44(1):42-49.
- [7] Faralli A, Giovannini N, Nardi S, et al. Indoor Real-Time Localisation for Multiple Autonomous Vehicles Fusing Vision, Odometry and IMU Data[M]// Modelling and Simulation for Autonomous Systems. 2016.
- [8] Aghili F, Su C Y. Robust Relative Navigation by Integration of ICP and Adaptive Kalman Filter Using Laser Scanner and IMU[J]. IEEE/ASME Transactions on Mechatronics, 2016, 21:1-1.
- [9] 张晗, 陈卫东, 王景川, 等. 多机器人探索系统的人机共享控制[J]. 机器人, 2015(1):17-24.
- [10] Eryildirim A, Guldogan M B. A Bernoulli Filter for Extended Target Tracking using Random Matrices in an UWB Sensor Network[J]. IEEE Sensors Journal, 2016, 16(11):1-1.
- [11] 王国胜, 夏凡, 吕强, 等. 基于动力学与运动学的四轮全向移动机器人轨迹跟踪控制[J]. 装甲兵工程学院学报, 2015(1):54-59.
- [12] DecaWave官方网站. <http://www.decawave.com/>
- [13] 阴盼强, 路东明, 袁渊, 等. 基于马氏距离的改进非局部均值图像去噪算法[J]. 计算机辅助设计与图形学学报, 2016, 28(3):404-410.
- [14] Rousseeuw P J, Driessen K V. A Fast Algorithm for the Minimum Covariance Determinant Estimator[J]. Technometrics, 1999, 41(3):212-22